Design and Characterization of the EP-Face Connector

Tarik Tosun, Jay Davey, Chao Liu, and Mark Yim

***Abstract*— We present the EP-Face connector, a novel connector for hybrid chain-lattice type modular robots that is high-strength (88.4N), compact, fast, power efficient, and robust to position errors.**

The connector consists of an array of electro-permanent magnets (EP magnets) embedded in a planar face. EP magnets are solid-state magnets that can be turned on and off and require power only when changing state.

In this paper, we present the design of the connector, manufacturing process, detailed experimental characterization of the connector strength under different loading conditions, and compare its performance to existing magnetic and mechanical connectors. We also illustrate the functional benefits of the EP-Face by demonstrating reconfiguration with the SMORES-EP robot.

I. INTRODUCTION

Modular reconfigurable robots are systems composed of a number of simple repeated robot modules that connect together to form larger robotic structures. Over several decades of research, dozens of different systems have been built [15], [20] and a wide range of functionality has been demonstrated, (including walking, grasping, and traversing obstacles) for applications ranging from search and rescue [18] to space exploration [19].

Self-reconfiguration is enabled by automatic connection mechanisms that allow these modules to attach and detach, and many of these systems use different methods for connection. There are a number of desirable qualitative and quantitative characteristic for a modular robot connector to have, including high strength, high speed of connection/disconnection, low power consumption, and large area-of-acceptance [4].

This paper introduces the EP-Face connector, which uses an array of four electro-permanent magnets mounted in a planar face to create a high-strength (88.4N) connection between modules. The connector is *fast* (connecting/disconnecting in 80 milliseconds), *compact* (low-profile, solid-state components), *robust* (large area-of-acceptance, self-aligning, genderless, rotationally symmetric, capable of docking from any approach direction), and *energy efficient* (requiring only 2.5 joules to switch states).

In this paper, we present the connector design, characterize it through experiments, and compare its performance with existing connector designs. In Section II, we provide an overview of existing modular robot connectors. In Section III-A, we present the connector design, as well as the manufacturing processes and fixtures used to construct hundreds of EP magnets. In Section IV, we characterize the connector through experiments. In Section V, we discuss our results and compare the connector with other systems. Finally, in Section VI, we discuss future work and conclude.

Tosun, Liu, and Yim: University of Pennsylvania, Philadelphia PA
Davey: Transcriptic, Menlo Park, CA

II. RELATED WORK

A. Electro-Permanent Magnets

An electro-permanent magnet consist of two permanent magnet rods with an electromagnet coil wrapped around them. Both rod magnets have the same remnant magnetization, but one has relatively low coercivity (polarization can be changed through exposure to a magnetic field) while the other has high coercivity (a much larger magnetic field is required to change polarization). A short pulse of current through the coil sets the polarization of the low-coercivity magnet, allowing magnetic force to be turned on or off (on when both are polarized the same way, off when opposite). Once set, polarization is maintained until another pulse is applied. The reader is referred to [10] for more information.

EP magnets have been used as connectors in lattice-type modular robots and programmable matter systems [9], [8], [6]. The Pebbles and Lily robots operate in a 2d lattice, and are primarily concerned with cluster self-assembly or self-dissassembly rather than strength. Their magnetic connectors withstand in-plane forces of $3.18N$ and $1.28N$, respectively. Each Pebble is 10mm long and weighs, 4.0g; each Lily is 35 mm long and weighs 26g [6], [8].

The EP-Face is component of SMORES-EP, a hybrid chain-lattice type modular robot, intended to form articulated chains that serve as bodies and legs as well as three dimensional lattices. SMORES-EP is much larger and heavier than the above systems, with a characteristic length of 80mm and a mass of 500g/module. As such, it has very different connector requirements. The EP-Face connector is expected to withstand forces on the order of tens of Newtons under normal, shear, and bending loading.

B. Modular Robot Connector Systems

A wide variety of connectors for hybrid modular robots can be found in the literature. Other systems that use magnets include MTRAN II [12] and the Telecubes system [16]. Telecubes and MTRAN II both exert connector forces of about $25N$ per magnet, about the same as the EP-Face ($28.3N$). Both use permanent magnets for latching, and disconnect them using shape-memory alloy (SMA) actuators. The disadvantages of SMA are its slow response time (it can take minutes to cool after heating), and notorious energy inefficiency. The EP-Face is able to switch the state of its EP magnets in 80 milliseconds with little energy ($2.5J$).

The MICHE robot [7] is a predecessor to the Pebbles, and uses mechanically switchable permanent magnet connectors that exert about 20N of force. The connectors control the flow of magnetic field by changing the relative orientation of two circular permanent magnets using a small gearmotor. The connector uses a small amount of energy, but requires room for the motor, has moving parts, and takes 1.3 seconds to switch states.

Structural hook-type connectors are popular for hybrid self-reconfigurable robots. Examples include the ATRON and MTRAN III robots [13], [11]. The advantage of these connectors is high strength: ATRON can theoretically support up to 800N before material failure. Compared to magnets, they sacrifice versatility and often require large amount of space. The majority of volume within each module of the ATRON was consumed by the connection mechanism [13]. They also tend to be mechanically complex, with many moving parts that can break or wear over time. The EP-Face connector is solid-state, requiring only a pulse of current to connect or disconnect.

The SINGO connector, developed for the Superbot robot, is more versatile [14]. It is hermaphroditic, and capable of disconnection even when one module is unresponsive, allowing for self-repair. However, it is mechanically complex, and sacrifices some strength for versatility.

The most natural point of comparison is its predecessor, the original SMORES robot connector [2], with four permanent magnets on a flat face and a mechanical key that enables latching and unlatching. The EP-Face is able to dock in a wider range of conditions than the original SMORES face. It is also stronger in normal loading than the SMORES face (85N compared to 60N), but weaker in shear (35N compared to (theoretically) 3.6kN).

A more detailed comparison of the EP-Face connector to existing connectors can be found in Section V.

III. Connector Design

A. Physical Design

The connector is shown in Figures 1 and 2. It consists of an array of 4 EP magnets arranged in a ring, with south poles counterclockwise of north. The ring arrangement of the magnets makes the connector hermaphroditic, and able to connect in four possible configurations. The magnets are held in place by glue, and externally protrude a distance of 0.5mm beyond the planar surface of the 3d-printed face. This way, the protruding magnets surfaces are the point of contact when connecting faces are brought together, minimizing the possibility of a detrimental air-gap between any pair of magnets.

Internally, leads from the magnets are soldered to a circuit board mounted above the magnets, which includes a microcontroller and driving circuitry, discussed in more detail in the following section. Measuring from the magnet face to the top of the circuit board, the total height of the EP-face connector is $16.6mm$. Measuring to the top of the slip ring canister, the total height is $19.6mm$.

Figure 3 shows the EP magnets. Each magnet consists of two cylinder magnets (AlNiCo 5 and NdBFe, both $4.76mm$ in diameter and $9.53mm$ long) and two identical pole pieces machined from ASTM 1018 Low-Carbon Steel. Mechanical constraints of the SMORES-EP module require that the magnet array fit within a 42mm diameter circular region. Machining the pole pieces into semicircles maximizes the allowable size of the EP magnets (if rectangular pole pieces were used, the corners would collide). The pole piece has a lip that sits on a corresponding ledge in the face, allowing the foot to protrude out of face by the prescribed amount and serving to transmit force on the magnet to the plastic face. Glue is used to hold the magnets in place in the face, but is not load-bearing.

The surface area of the pole pieces is critical to the strength of the magnetic force. Magnetic force per area is proportional to flux density squared. Therefore, decreasing pole area increases holding force, but only up to the saturation density of low-carbon steel ($1.5T$). Based on the diameter and average magnetic flux density of the permanent magnet cylinders ($1.38T$ for both NdBFe and AlNiCo), the minimum contact area of the steel pole piece was found to be $32.7mm^2$. The actual semicircular contact surfaces of the poles have an area of $33mm^2$. Based on these values, the theoretical maximum holding force is $46N$ per magnet or $184N$ per EP-face.

The solenoid coil was designed to generate sufficient magnetic field intensity for the AlNiCo magnet to reach saturation. Using the method described by Knaian [10], this was found to be 200 turns of AWG 40 wire.

B. Manufacturing

Here we provide an overview of the EP-Face manufacturing process. More details can be found at http://www.modlabupenn.org/ep-face.

At the time of writing, we have built 14 SMORES-EP modules, 70 EP-faces, and over 300 EP magnets, with the eventual goal of building 30 modules (120 EP-Faces, 480 magnets). The primary manufacturing challenge was ensuring that all pole pieces in an EP-face were aligned into a perfectly flat plane. Misaligned pole pieces have less contact surface area with mated magnets, which can significantly reduce connection strength.

Pole pieces were machined from 0.25x0.5in 1018 Low-Carbon Steel rod stock. Edges were deburred manually and smoothed in a vibratory tumbler overnight. Smoothing was important because sharp pole edges can scrape off wire enamel during the winding process, causing shorts within a magnet.

EP magnets were mechanically assembled using high-viscosity cyanoacrylate glue in a custom 3d-printed fixture shown in Figure 4. Pole pieces and magnet cylinders are vertically clamped, fully constraining motion except for travel along the rails. This gluing process was the most error-prone part of manufacturing, mostly due to glue residue buildup in the fixture. Misaligned magnets (Fig. 5) were bathed in solvent and recycled.

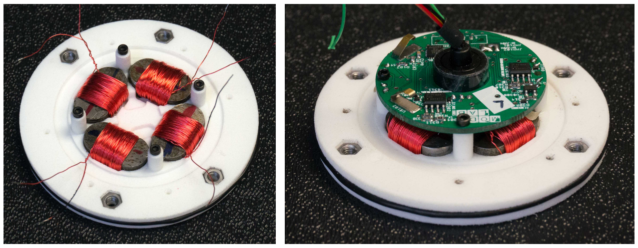

Fig. 1: Left: Internal view of magnets in EP-Face. Right: Internal view of EP-face with circuit board and slipring.

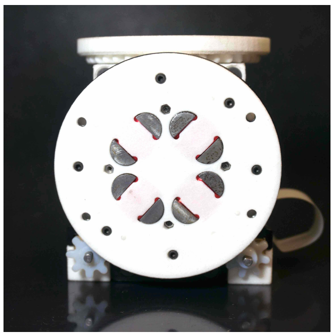

Fig. 2: EP-face on a SMORES-EP module.

Magnets were wound in a purpose-built machine constructed from Lego Mindstorms (Figure 4). Wound magnets were verified by checking resistance (nominally 2.08 Ohms, with lower resistance indicating an internal short), and testing strength (must lift a 2kg steel block when activated manually using a power supply at 11V).

To construct the EP-face, four magnets are inserted into their slots in 3d-printed face. The face is placed on a perfectly flat steel block, and all magnets are activated, forcing them to align to the steel surface as closely as possible. The face is lifted, and if it supports a suspended 5kg load, it is considered up-to-spec. The magnets are fixed in place with glue, and remain attached to the steel surface until the glue cures.

C. Electrical Design

1) Driving Circuitry: The four EP magnets in an EP-face are driven by an array of five half-H bridges (Fairchild FDS8958B), capable of sourcing the 6 amps required to activate and deactivate the EP magnets. As shown in Figure 6, one side of each magnet is connected to a dedicated half-H bridge, while the other side is connected to a common half-H bridge shared between all the magnets. This circuit allows bi-directional drive of each magnet, as long as only one magnet is fired at a time. Similar driving circuits are used in [6] and [8].

The array of half-H bridges is controlled by an ATMega 168a microcontroller with 16kb of flash memory, 512kb EEPROM, and 1Kb internal SRAM running at 8Mhz. To activate or deactivate a magnet, three pulses of length 3ms are applied at intervals of 3ms. The magnets are fired at battery voltage (between 11.1V and 12.6V depending on charge). A voltage regulator and capacitor could have been used to provide more consistent firing voltage. The authors chose to omit these components due to tight space requirements, but recommend that others consider them in their own designs.

2) Inductive Communication: Connected EP-faces can exchange data through the magnetic coupling of connected EP-magnets: when a coil is pulsed, the generated magnetic field also flows through the core of the connected coil, and the changing field generates a voltage across that coil. Through this channel, EP-faces are capable of UART serial communication. Similar capabilities have been demonstrated in [6] and [8].

D. Integration with the SMORES-EP Module

The EP-face and driving circuitry form a compact self-contained unit with no moving parts (Figure 1). The microcontroller associated with each driver array is configured as an I2C peripheral, and receives commands from the main microcontroller on the module motherboard.

The electrical interface between each EP-face and the rest of the module consists of five lines: High power (battery voltage), logic power (+3.3v), I2C clock, I2C data, and ground. Because the mechanical design of SMORES-EP

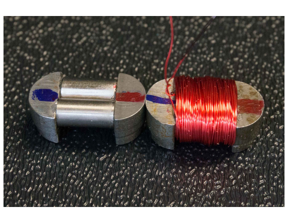

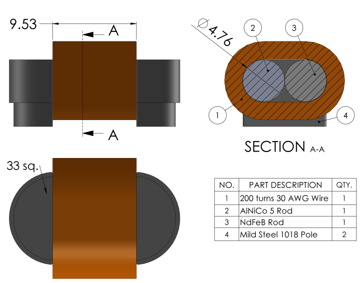

NO.	PART DESCRIPTION	QTY.
1	200 turns 30 AWG Wire	1
2	AlNiCo 5 Rod	1
3	NdFeB Rod	1
4	Mild Steel 1018 Pole	2

Fig. 3: Left: EP magnets, before and after winding. Right: Technical drawing of EP magnet, dimensions in millimeters.

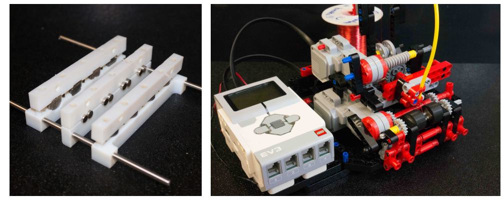

Fig. 4: Gluing fixture (left) and winding machine (right)

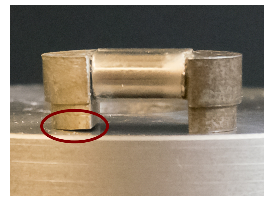

Fig. 5: Misaligned EP magnet. The left pole (circled in red) makes contact on its edge rather than its face, reducing contact surface area and flux transmission.

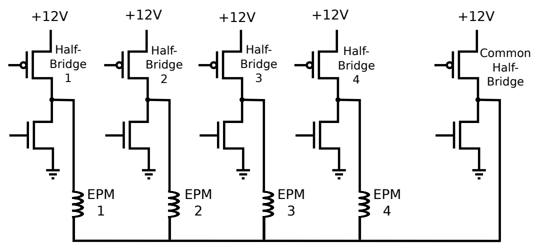

Fig. 6: Circuit for Driving EP Magnets.

requires the top and side faces to rotate continuously, these three faces are connected to the central electronics via slip rings (Senring SNM012U-06) mounted in the middle of the face.

The bottom face of SMORES-EP does not rotate continuously, so it does not need a slip ring. Instead, the circuit board is located in the center of the module, and connected to the bottom face magnets through a ribbon cable.

IV. Experimental Results

A. EP Magnet Characterization

1) Holding Force in Normal Loading: The holding force of a pair of EP magnets was characterized using a materials testing machine (MTS) to generate stress/strain plots. In each trial, both magnets were activated by manually pulsing current from a power supply set to 12V. Four pairs of magnets were tested, with five trials per pair. The maximum holding force was 39N, and the average was 28.3N with a standard deviation of 5.2N.

2) Normal force as function of air gap at firing: The holding strength of an EP magnet is significantly higher when pulsed in contact with another magnet (or ferromagnetic object) than when pulsed in free air. This is because the air forms a magnetic circuit with higher total reluctance, reducing the peak field in the circuit and therefore also reducing the magnetization of the AlNiCo magnet. As mentioned in Section III-B, misaligned pole pieces result in a similar effect.

In this experiment, we characterize the holding force of the magnets as a function of air gap at firing. One pair of magnets was tested. At the beginning of each trial, both magnets were manually deactivated using a power supply. Paper shims were used to create well-controlled effective "air gap" between magnets[1]. Both magnets were fired three times with the paper spacer in place. The paper was slid out from between the magnets and measured, the magnets were placed in contact, and a loading test was performed.

Figure 8 plots holding force against gap at firing. Force decreases rapidly with increasing gap distance, and the dropoff is sharp for small gaps. At a gap distance of 0.25mm, holding force is reduced to half of the value with magnets in contact.

[1]We assume the magnetic permeabilities of paper and air are similar. The magnetic permeabilities of nearly all non-ferrous substances (such as paper and air) differ by much less than one percent [1].

B. EP-Face Characterization

1) Normal Loading: In this experiment we characterize the holding force of an EP-face. In each trial, faces were aligned and placed in contact, and then magnets were fired three times. Nine pairs of faces were tested. Each pair of faces was rotated through all four possible connection orientations, and five trials were performed for each orientation. By using a large sample size, we capture the variability in holding strength, which is functionally important because the capability of a cluster is limited by the strength of its weakest connector (if one connection breaks, the cluster cannot perform as intended).

The maximum holding force was 115N, and the average was 88.4N with a standard deviation of 13.9N. Figure 9 shows a histogram of holding forces for this experiment. We believe the large variability in holding force is due to the fact that each face-to-face connection consists of four magnet-to-magnet connections, and when loaded in the normal direction, failure of the single weakest magnet-to-magnet connection will cause the entire face-to-face connection to fail. We hypothesize that many of the low-force failures are due to poor contact between a single mated pair of magnets on connected faces, creating a "weakest link" that lowers performance. This is supported by the data: the average standard deviation for a given orientation (pairing of magnets)[2] is 6.13N, while the average standard deviation of all trials for a given face pairing[3] is 10.4N.

2) Effect of Battery Voltage: Magnetization of the AlNiCo magnet depends on the strength of the field created by the coil during pulsing. Since the magnets are fired at battery voltage, changes in battery voltage during operation of a module affects the strength of the magnets. Holding force under normal loading was tested at firing voltages ranging from 9 to 16 volts, using a power supply capable of sourcing sufficient current.

Figure 10 shows the results of these tests. We see a clear trend of increasing holding force with increasing supply voltage, with the curve leveling off around 14V, indicating that the AlNiCo magnetization has saturated. In normal operation, a SMORES-EP module has battery voltage between 12.6V and 11V.

3) Shear: Holding force under shear loading was tested by connecting two modules side-by-side and pulling one upward (fixture shown in Figure 7). Eight pairs of faces were tested, with five trials performed for each pairing. Different orientations of the pairings were not tested.

The maximum holding force in shear was 41N, and the average was 28.4N with a standard deviation of 6.39N. Figure 11 shows force versus displacement during one of the trials. Two distinct regimes are visible. First, there is a smooth rapid rise in force, due to static friction between the pole pieces. After static friction is overcome (26.52N), force

[2]Standard deviation of the 5 trials per orientation, averaged over 36 total orientations (4 orientations$\times$9 pairings). In a given orientation, the same pairs of magnets are mated in each trial.

[3]Standard deviation of the 20 trials (5 trials$\times$4 orientations) per face pairing, averaged over 9 face pairings.

continues to increase as the magnets are pulled away from each other, until failure occurs at 31.8N.

4) Bending (Characteristic Strength): Bending strength was tested by connecting two modules side-by-side and pulling upward on a lever mounted on the side of one module. One pair of modules was tested at a battery voltage of $12.6V$, with five trials done at each of four lever lengths. The average failure moment at the connected face was $1.8Nm$. Since the SMORES-EP module mass is $0.454kg$ and module length is $81mm$ from magnet to magnet, this is an equivalent load to supporting 3.1 modules in cantilever. This number is used as a figure of merit for modular robots, called *characteristic strength* [5]. In practice, due to variability of connection strength and inertial moments when moving, the functional limit for cantilever structures is two modules in most applications.

5) Torsion: Torsional strength was tested in a manner similar to bending, except that the modules were mounted so that pulling up on the lever twisted one face relative the other. The average failure moment about the center of the connected faces was $0.83Nm$.

6) Normal and Parallel Offset Area-of-Acceptance: To test the connection tolerance to offsets in the direction normal and parallel to the connected faces, two modules were positioned offset from one another with bottom faces sitting flat on a table (with magnets turned off), and the magnets were turned on. This process was repeated with decreasing gap distance until force at magnet activation was sufficient to draw the modules together (demonstrated in the accompanying video).

Magnetic forces can draw two modules together through a gap of 4mm (normal to the faces), and 7mm parallel to the face. The coefficient of friction between the modules and table was experimentally determined to be 0.15.

7) Rotational Area-of-Acceptance: To test the rotational area of acceptance of the faces, we tested the normal direction breakage strength when the two faces were misaligned. The jig shown in Figure 7 rigidly fixes both the position and orientation of the modules to the clamps of the MTS machine, allowing the connecting faces to be held at a controlled angular offset relative one another.

In each trial, the magnets were first deactivated three times to eliminate any residual magnetization from past trials. The faces were then placed in contact, with a measured angular offset. The magnets were fired three times, and normal load was applied until failure. One pair of faces was tested at three offset angles, with five trials at each offset angle. Figure 12 plots normal holding force against angular offset. Normal force decreases linearly with angular offset, retaining about 10% of the zero-offset value by 25 degrees. Assuming bending strength scales with normal strength, the EP-face can still support one module in cantilever at an offset of 25 degrees (bending failure is $1.8Nm$, and one cantilevered module is $0.19Nm$).

8) Time and Energy: When an EP-Face is turned on (magnetized) or off (demagnetized), each magnet takes $20ms$ to fire ($9ms$ of current pulses, $11ms$ of wait time). To change

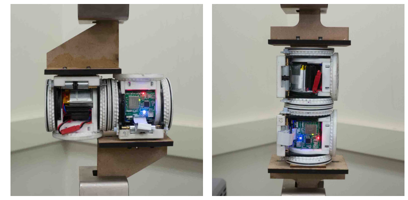

Fig. 7: (Left) Shear and (Right) Angular Offset test setups

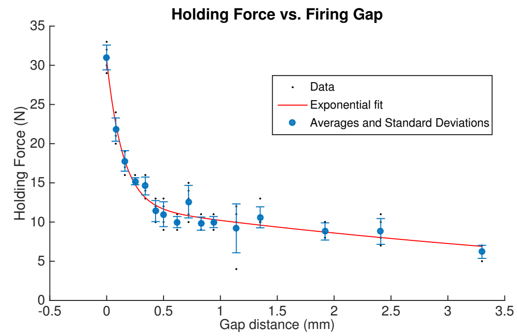

Fig. 8: Plot of Holding Force vs. Gap at Firing. Exponential fit: $y = 18.63\exp(-7.019x) + 12.08\exp(-0.1697x)$

the state of an entire face, this requires $80ms$. Assuming a nominal $12V$ battery voltage and 2.08Ω resistance, the peak power consumption is $69.23W$, and the total switching energy is $2.5J$ per face.

V. Discussion

A. Advantages

The EP-Face has a number of desirable qualities. Connection and disconnection are nearly instantaneous, requiring only $160ms$ for a connect-disconnect cycle. Most other connectors require time on the order of seconds or minutes (Table I). The energy required is also small, $2.5J$ per state-change, as compared to $3.75J$ for the SINGO connector

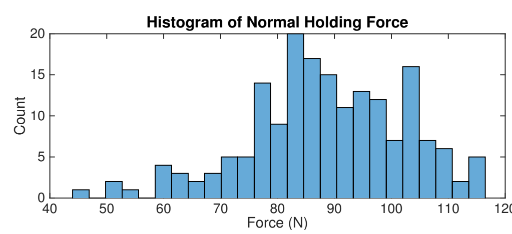

Fig. 9: Histogram of Holding Forces Under Normal Load. Mean=88.4N, Std=13.9N.

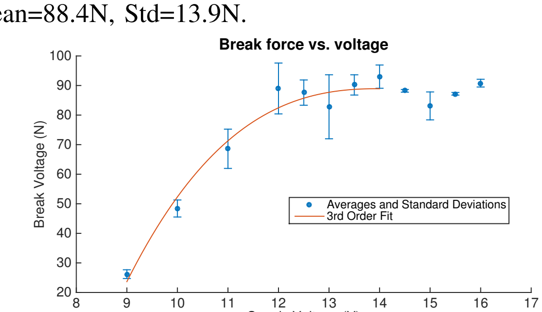

Fig. 10: Face Break Force vs. Supply Voltage. Cubic fit: $y = 0.313x^3 - 14.3x^2 + 215x - 981$

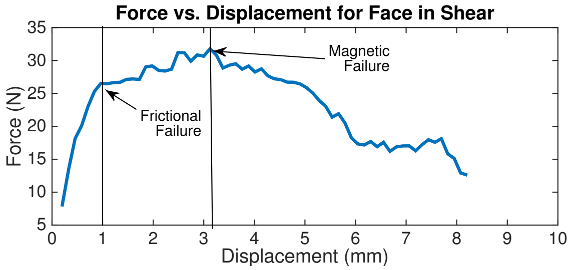

Fig. 11: Force vs. displacement in shear. Peak force of 31.8N at displacement of 3.1mm. Note while static friction failure appears to occur at a displacement of 1mm, this large displacement is due to deformation (slop) of the module, not movement of the magnets.

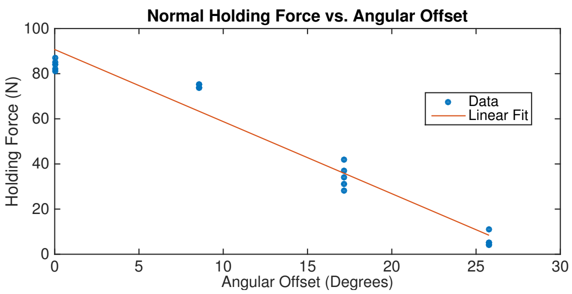

Fig. 12: Normal Holding Force vs. Angular Offset. Linear fit: $y = -3.194x + 90.7$

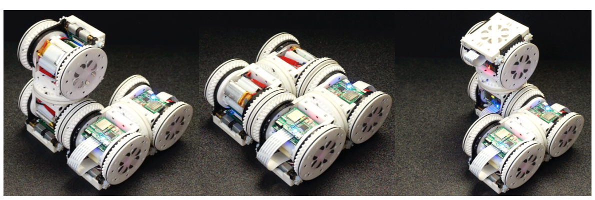

Fig. 13: Slide-by docking is made possible by the thin profile of the EP-Face.

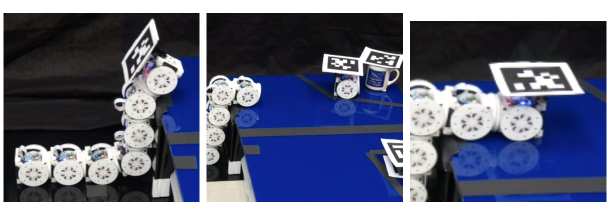

Fig. 14: Ledge exploration. (Left) Seven-module snake lifts its head to the top of a 3-module high ledge. (Center) Head module detaches, and explores the surface. (Right) Head module autonomously reattaches, and snake descends.

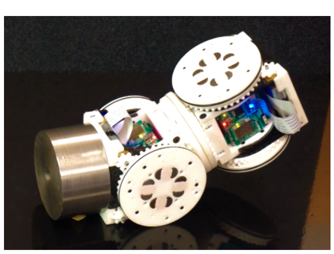

Fig. 15: SMORES-EP module moving a 1kg metal block while lifting another module in the air.

[14]. The time and energy costs of EP-Face connection are vanishingly small in comparison with movement actions SMORES-EP can perform.

The forces supported by EP-faces are comparable to other magnetic connectors (Table I), and sufficient to perform tasks such as ledge climbing (Fig. 14). Under normal loading, it supports the weight of 17 modules. Additionally, since the connection is magnetic, SMORES-EP modules have demonstrated the ability to manipulate ferrous objects as heavy as 1kg (Figure 15).

The connector is low-profile, with the magnets protruding only $0.5mm$ from the face. The interior thickness is also small (magnets are 10.2mm tall, and total thickness including slip ring is 20mm). Many existing connectors are thicker, sometimes comprising a significant fraction of the total module volume (ATRON, SMORES [13], [2]).

Latching and unlatching actions require no moving parts, and impose no constraints on module movement. Many other connectors are mechanically complex, with moving parts that can break or wear over time (ATRON, SMORES, SINGO, MTRANvIII [13], [2], [14], [11]). Additionally, while mechanical latches are usually stronger than magnetic connections, overloading can result in plastic deformation or fracture, permanently damaging the connector. In this sense, magnetic connections are more robust to overloading, allowing for the possibility of re-connecting after being overloaded.

Connectors with interlocking external features often require a specific angle of approach to connect. For example, the SINGO (SuperBot) and PolyBot connectors would not be capable of the kind of slide-by docking demonstrated by SMORES-EP in Figure 13, because their protruding features would collide [14], [3]. Similarly, the original SMORES connector cannot reliably perform slide-by docking because the permanent magnets get stuck in a local minimum configuration before the faces are actually mated. Because the EP-Face magnets lie in a single plane and can be switched off, there is no dependence on approach angle for docking; whe two faces can be brought into contact, they can connect.

EP-Faces do not need to be perfectly aligned to connect successfully; the connector has a forgiving area of acceptance. As presented in the prev ious section, latching forces can draw two two modules together through a gap of 4mm (normal to the faces), and 7mm parallel to the face. Even if the faces are held with an angular misalignment of 25 degrees, the connection is strong enough to support the weight of one module. This can be compared to the tolerances of SINGO (max 6mm normal, 5mm parallel, or 5.7 degrees) and MTRANIII (max 2mm normal, 5mm parallel, or 10 degrees). The EP-Face is hermaphroditic and rotationally symmetric, with a pair of faces able to connect in four different orientations (0, 90, 180, and 270 degrees relative one another).

B. Disadvantages

With no mechanical features on the connection plane, shear loading is supported by static friction and magnetic restoring forces. Connector strength is significantly weaker under shear and torsional loading than normal loading.

The magnetic connection is also somewhat compliant, especially in shear and torsion. In the force vs. displacement plot for shear (Figure 11), we see a displacement of three millimeters before the maximum force is reached.

Connection strength is significantly affected by air gap when the magnets are fired, as demonstrated in the experiments. Fortunately, in some circumstances this is mitigated by the self-aligning properties and low cost of connection: once the magnets establish a weak connection, they can be fired again to strengthen the connection.

Because of this air gap sensitivity, the system needs to run in relatively clean environments. Outdoor environments with dirt and other debris that may be collected or stick to the magnet faces may reduce connection strength.

Some systems (such as SINGO [14]) are able to disconnect even if one module is unresponsive, facilitating removal of the broken module from the cluster. The EP-Face cannot do this: if one module becomes unresponsive with its magnets switched on, they will exert a holding force even if a connected module switches its magnets off.

VI. Conclusions and Future

We introduced and characterized the EP-Face, an EP magnet-based connector for the SMORES-EP robot. We discussed its advantages relative to existing connectors, most notably its compactness, very fast connection speed (80ms) and wide area of acceptance. We also demonstrated how the EP-Face allows the SMORES-EP module to reconfigure and interact with its environment.

Overall, we think the advantages of the EP-Face make it a good option for modular robots the size of SMORES-EP. The main avenue of future work will be exploring ways to increase the shear and torsional strength of the connector. It may be possible to increase strength by adding a friction-enhancing surface finish to the faces. Another option is the addition of surface features that interlock to resist shear and torsion. Unidirectional features (alternating ridges and valleys in one dimension) could increase strength while still allowing slide-by docking.

Connector	**EP face**	**SMORES**	**SINGO**	**ATRON**	**MTRAN 3**	**MTRAN 2**	**PolyBot 2**
Type	EP Mag	Mag /Mech	Mech	Mech	Mech	Mag/ SMA	Mech/ SMA
Thickness (mm)	16.6	50	24*	50*	20*	20*	9.5
Gender	H	H	H	G	G	G	H
Orientations	4	2	4	1	4	2	4
Connection Cycle Time	160ms	2.3s	50s	4s	5s	30s	30s
Char. Strength	3.1	3	3.7	2.58	-	2.59	6.14
Connection Energy (Joules)	2.5	< 5*	3.75	< 5*	< 5*	200*	> 100*
Citation	-	[2]	[14]	[13]	[11]	[12]	[3]

Notes: H/G= Hermaphroditic/Gendered, *=approx,
Green=Best, Red=Worst, Characteristic strength values from [17].
SINGO thickness includes estimated 10mm for motor.

TABLE I: Comparison of Connectors

Acknowledgments

The authors would like to thank the large and talented team of students who contributed to this project. In particular, Thulani Tsabedze, Matt Oslin, Gabrielle Merritt, and Daniel Edgar deserve special thanks. This work was funded by NSF grant numbers CNS-1329620 and CNS-1329692.

References

[1] Magnetic properties of materials. http://info.ee.surrey.ac.uk/Workshop/advice/coils/mu/. Accessed: 2016-02-20.

[2] Jay Davey, Ngai Kwok, and Mark Yim. Emulating self-reconfigurable robots-design of the smores system. In *IROS*. IEEE, 2012.

[3] David Duff, Mark Yim, and Kimon Roufas. Evolution of polybot: A modular reconfigurable robot. In *Proc. of the Harmonic Drive Intl. Symposium, Nagano, Japan*. Citeseer, 2001.

[4] Nick Eckenstein and Mark Yim. The x-face: An improved planar passive mechanical connector for modular self-reconfigurable robots. In *IROS*. IEEE, 2012.

[5] Nick Eckenstein and Mark Yim. Modular advantage and kinematic decoupling in gravity compensated robotic systems. *Journal of Mechanisms and Robotics*, 5(4):041013, 2013.

[6] Kyle Gilpin, Ara Knaian, and Daniela Rus. Robot pebbles: One centimeter modules for programmable matter through self-disassembly. In *ICRA*. IEEE, 2010.

[7] Kyle Gilpin, Keith Kotay, Daniela Rus, and Iuliu Vasilescu. Miche: Modular shape formation by self-disassembly. *The International Journal of Robotics Research*, 27(3-4):345–372, 2008.

[8] Bahar Haghighat, Emmanuel Droz, and Alcherio Martinoli. Lily: A miniature floating robotic platform for programmable stochastic self-assembly. In *ICRA*. IEEE, 2015.

[9] Ara N Knaian et al. The milli-motein: A self-folding chain of programmable matter with a one centimeter module pitch. In *IROS*. IEEE, 2012.

[10] Ara Nerses Knaian. *Electropermanent magnetic connectors and actuators: devices and their application in programmable matter*. PhD thesis, Citeseer, 2010.

[11] Haruhisa Kurokawa et al. Distributed self-reconfiguration of m-tran iii modular robotic system. *IJRR*, 2008.

[12] Satoshi Murata et al. M-tran: Self-reconfigurable modular robotic system. *Mechatronics, IEEE/ASME Trans.*, 2002.

[13] Esben Hallundbæk Østergaard, Kristian Kassow, Richard Beck, and Henrik Hautop Lund. Design of the atron lattice-based self-reconfigurable robot. *Autonomous Robots*, 21(2):165–183, 2006.

[14] Wei-Min Shen, Robert Kovac, and Michael Rubenstein. Singo: a single-end-operative and genderless connector for self-reconfiguration, self-assembly and self-healing. In *ICRA*. IEEE, 2009.

[15] Kasper Stoy, David Brandt, David J Christensen, and David Brandt. *Self-reconfigurable robots: an introduction*. Mit Press Cambridge, 2010.

[16] John W Suh, Samuel B Homans, and Mark Yim. Telecubes: Mechanical design of a module for self-reconfigurable robotics. In *ICRA*. IEEE, 2002.

[17] Paul Joseph White. Miniaturization methods for modular robotics: External actuation and dielectric elastomer actuation. 2011.

[18] Mark Yim, David G Duff, and Kimon Roufas. Modular reconfigurable robots, an approach to urban search and rescue. In *Proc. 1st Intl. Wkp. on Human-friendly Welfare Robotics Systems, Taejon, Korea*, 2000.

[19] Mark Yim et al. Modular reconfigurable robots in space applications. *Autonomous Robots*, 14(2-3):225–237, 2003.

[20] Mark Yim et al. Modular self-reconfigurable robot systems [grand challenges of robotics]. *Robotics & Automation Magazine, IEEE*, 14(1):43–52, 2007.